






ORIGINAL RESEARCH

# Antiatherosclerotic Phenotype of Perivascular Adipose Tissue Surrounding the Saphenous Vein in Coronary Artery Bypass Grafting

Takuma Mikami , MD\*; Masato Furuhashi , MD, PhD\*; Akiko Sakai, MSc; Ryosuke Numaguchi , MD, PhD; Ryo Harada, MD, PhD; Syuichi Naraoka, MD, PhD; Takeshi Kamada, MD, PhD; Yukimura Higashiura, MD; Marenao Tanaka, MD, PhD; Shunsuke Ohori, MD; Taku Sakurada, MD, PhD; Masanori Nakamura, MD, PhD; Yutaka Iba , MD, PhD; Joji Fukada, MD, PhD; Tetsuji Miura , MD, PhD; Nobuyoshi Kawaharada, MD, PhD

**BACKGROUND:** Perivascular adipose tissue (PVAT) is associated with metabolically driven chronic inflammation called metaflammation, which contributes to vascular function and the pathogenesis of vascular disease. The saphenous vein (SV) is commonly used as an essential conduit in coronary artery bypass grafting, but the long-term patency of SV grafts is a crucial issue. The use of the novel “no-touch” technique of SV harvesting together with its surrounding tissue has been reported to result in good long-term graft patency of SV grafts. Herein, we investigated whether PVAT surrounding the SV (SV-PVAT) has distinct phenotypes compared with other PVATs of vessels.

**METHODS AND RESULTS:** Fat pads were sampled from 48 patients (male/female, 32/16; age, 72±8 years) with coronary artery disease who underwent elective coronary artery bypass grafting. Adipocyte size in SV-PVAT was significantly larger than the sizes in PVATs surrounding the internal thoracic artery, coronary artery, and aorta. SV-PVAT and PVAT surrounding the internal thoracic artery had smaller extents of fibrosis, decreased gene expression levels of fibrosis-related markers, and less metaflammation, as indicated by a significantly smaller extent of cluster of differentiation 11c–positive M1 macrophage infiltration, higher gene expression level of adiponectin, and lower gene expression levels of inflammatory cytokines, than did PVATs surrounding the coronary artery and aorta. Expression patterns of adipocyte developmental and pattern-forming genes were totally different among the PVATs of the vessels.

**CONCLUSIONS:** The phenotype of SV-PVAT, which may result from inherent differences in adipocytes, is closer to that of PVAT surrounding the internal thoracic artery than that of PVAT surrounding the coronary artery or that of PVAT surrounding the aorta. SV-PVAT has less metaflammation and consecutive adipose tissue remodeling, which may contribute to high long-term patency of grafting when the no-touch technique of SV harvesting is used.

**Key Words:** coronary artery bypass surgery ■ epicardial fat ■ perivascular fat ■ saphenous vein

**P**erivascular adipose tissue (PVAT) plays a role in supporting vascular structure and metabolism, and it contributes to vascular function and the pathogenesis of vascular disease.<sup>1</sup> PVAT is implicated

in the regulation of vascular tone by releasing adipose-derived relaxing and contracting factors, which contribute to the protection and progression of atherosclerotic vascular disease.<sup>2–5</sup> It has been reported that epicardial

Correspondence to: Masato Furuhashi, MD, PhD, Department of Cardiovascular, Renal and Metabolic Medicine, Sapporo Medical University School of Medicine, S-1, W-16, Chuo-ku, Sapporo 060-8543, Japan. E-mail: furuhashi@sapmed.ac.jp

\*T. Mikami and M. Furuhashi contributed equally.

Supplementary Material for this article is available at <https://www.ahajournals.org/doi/suppl/10.1161/JAHA.120.018905>

For Sources of Funding and Disclosures, see page 11.

© 2021 The Authors. Published on behalf of the American Heart Association, Inc., by Wiley. This is an open access article under the terms of the Creative Commons Attribution-NonCommercial-NoDerivs License, which permits use and distribution in any medium, provided the original work is properly cited, the use is non-commercial and no modifications or adaptations are made.

JAHA is available at: [www.ahajournals.org/journal/jaha](http://www.ahajournals.org/journal/jaha)

## CLINICAL PERSPECTIVE

### What Is New?

- Perivascular adipose tissue surrounding the saphenous vein had less metabolically driven chronic inflammation called metaflammation, smaller extents of fibrosis, and decreased gene expression levels of inflammatory and fibrosis-related markers than did perivascular adipose tissue surrounding the coronary artery and that surrounding the aorta.
- The phenotype of perivascular adipose tissue surrounding the saphenous vein was close to that of perivascular adipose tissue surrounding the internal thoracic artery, an atherosclerosis-resistant vessel.

### What Are the Clinical Implications?

- The phenotype of perivascular adipose tissue surrounding the saphenous vein might be linked to the high rate of long-term patency of coronary artery bypass grafting using the “no-touch” technique of saphenous vein harvesting together with its surrounding tissue and intact endothelium.

## Nonstandard Abbreviations and Acronyms

<b>Ao-PVAT</b>	perivascular adipose tissue surrounding the aorta
<b>ASC</b>	apoptosis-associated speck-like protein containing caspase recruitment domain
<b>CA-PVAT</b>	perivascular adipose tissue surrounding the coronary artery
<b>CHOP</b>	C/EBP homologous protein
<b>GRP78</b>	glucose-regulated protein 78
<b>ITA</b>	internal thoracic artery
<b>ITA-PVAT</b>	perivascular adipose tissue surrounding the internal thoracic artery
<b>MCP-1</b>	monocyte chemoattractant protein-1
<b>PVAT</b>	perivascular adipose tissue
<b>SV</b>	saphenous vein
<b>SV-PVAT</b>	perivascular adipose tissue surrounding the saphenous vein

adipose tissue is a source of inflammatory mediators<sup>6</sup> and that an elevated volume of PVAT surrounding the coronary artery (CA-PVAT) is strongly associated with coronary atherosclerosis<sup>7–9</sup> and vasospastic angina<sup>10</sup> in combination with metabolically driven chronic inflammation called metaflammation<sup>11</sup> and an imbalance of cytokines and adipokines.

The internal thoracic artery (ITA) is protected from the development of atherosclerosis<sup>12</sup> and is frequently used as the gold standard graft material for coronary artery bypass grafting (CABG) because of its excellent long-term patency.<sup>13</sup> It has been reported that the ITA has less concentric atheromatous intimal thickening involving the whole circumference than does the right gastroepiploic artery, a candidate of graft vessels for CABG, even in patients with several coronary risk factors.<sup>14</sup> Furthermore, excellent endothelial function, including shear stress sensing and generation of NO and antithrombotic factors, of the ITA has been reported to provide physiological and metabolic effects that are beneficial in both the graft and recipient coronary artery.<sup>12,13</sup> We previously proposed that PVAT surrounding the ITA (ITA-PVAT) is protected from metaflammation and consecutive adipose tissue remodeling, possibly contributing to the decreased atherosclerotic plaque burden in the ITA.<sup>15</sup>

The saphenous vein (SV) is still commonly used as an essential conduit in CABG. However, the long-term patency of an SV graft is one of the most crucial issues in cardiovascular surgery.<sup>13</sup> It has recently been proposed that the “no-touch” technique should be used to harvest a complete SV together with its surrounding tissue and intact endothelium.<sup>16</sup> The use of the novel no-touch technique of SV harvesting has been reported to result in superior short- and long-term graft patency rates than those achieved by using the conventional technique of SV harvesting, and the rates were comparable to those for ITA grafts.<sup>17–19</sup> Supply of nutrients and oxygen to the SV wall and its surrounding tissue, including the vasa vasorum,<sup>20</sup> and preservation of endothelial integrity and luminal NO synthase derived from the intact endothelium<sup>21,22</sup> have been proposed as possible mechanisms of the benefit of the no-touch technique.

PVAT can be a source of several vasoactive factors.<sup>23,24</sup> However, the difference between PVAT surrounding the SV (SV-PVAT) and other PVATs of vessels remains unclear. We hypothesized that SV-PVAT has less metaflammation and smaller extents of fibrosis than do other PVATs of vessels, possibly contributing to the protection against atherosclerotic plaque burden in the vessel when no-touch SV is used as a graft material in CABG. In the present study, we investigated whether SV-PVAT, ITA-PVAT, CA-PVAT, and PVAT surrounding the aorta (Ao-PVAT) have distinct histological and gene expression phenotypes and functional relevance to vascular remodeling in patients with coronary artery disease who have undergone elective CABG.

## METHODS

This study conformed to the principles outlined in the Declaration of Helsinki and was performed with the approval of the Ethical Committee of Sapporo

Medical University (No. 312-34). Written informed consent was received from all of the study subjects. The data that support the findings of this study are available from the corresponding author on reasonable request.

## Study Patients

Patients diagnosed with coronary artery disease who underwent elective CABG surgery were consecutively recruited from Sapporo Medical University Hospital and the affiliated Hokkaido Ohno Memorial Hospital, Sapporo Central Hospital, Sapporo City General Hospital, Teine Keijinkai Hospital, and Otaru City General Hospital from March 2018 through March 2020. Patients treated with hemodialysis and those who underwent CABG without using the SV were excluded. The patients in the present study were not overlapped with the patients in our previous study in which PVAT was investigated.<sup>15</sup>

## Collection of Fat Pads

Fat pads of SV-PVAT from the area of the lower thigh SV, ITA-PVAT from the area of the left ITA, CA-PVAT from the area of the left coronary artery, and Ao-PVAT from the area of the ascending aorta were collected during surgery before anticoagulation and establishment of extracorporeal circulation. The samples were divided into 2 parts. The first specimen was stored in formalin and embedded in paraffin for histological staining, and the second specimen was frozen in liquid nitrogen for mRNA isolation and real-time polymerase chain reaction (PCR).

## Histological Analysis

Samples of fat pads were fixed in 10% formalin solution, dehydrated, and embedded in paraffin. Serial 5- $\mu$ m-thick sections were prepared, mounted onto glass slides, deparaffinized, and rehydrated through degraded ethanol. Tissues were stained with hematoxylin-eosin and Masson trichrome reagents. Immunohistochemical 3,3'-diaminobenzidine staining using mouse anti-cluster of differentiation (CD) 68 (Dako, Santa Clara, CA), rabbit anti-CD11c (Abcam, Cambridge, UK), and mouse anti-CD206 (Abnova, Taipei, Taiwan) antibodies was performed as previously described.<sup>15,25,26</sup> Control experiments were performed by omitting the primary antibodies or adding goat anti-mouse or goat anti-rabbit immunoglobulins (Dako) for control primary antibodies (Figure S1).

## Quantitative Image Analysis

Images were captured with a microscope (BZ-X700; Keyence, Osaka, Japan). Image analyses were performed using ImageJ and Fiji software.

The cross-sectional area of an adipocyte in hematoxylin-eosin staining was determined by calculating the mean area of 100 randomly selected adipocytes per optical field at  $\times 200$  magnification. The results were averaged, and they are expressed as adipocyte size ( $\mu\text{m}^2$ ). After checking sections of hematoxylin-eosin staining to avoid nonspecific fibrosis staining in the adventitia, sections were chosen to stain the fibrosis area in the inside, but not the edge, of adipose tissues. Fibrosis was assessed in Masson trichrome-stained tissue sections by quantifying the blue area representing collagen relative to the total tissue area at  $\times 100$  magnification. Furthermore, macrophage infiltration in tissue sections was assessed by quantifying the area stained by anti-CD68, CD11c, or CD206 antibodies relative to the total tissue area at  $\times 200$  magnification. For each quantitative analysis of fibrosis and macrophage infiltration, 3 randomly selected optical fields were examined per adipose tissue depot, and the results were averaged. Results are expressed as percentage positive area per total area. All of the measurements were performed in a double-blind manner by 2 different researchers.

## Quantitative Real-Time PCR

Total RNA was isolated from samples using the miRNeasy Micro Kit (QIAGEN, Hilden, Germany) and the RNase-Free DNase Set (QIAGEN). The amount and quality of isolated RNA were determined spectrophotometrically using Nanodrop (Thermo Fisher Scientific, Waltham, MA), and 500 ng of total RNA was reverse transcribed by using the high-capacity cDNA archive kit Reverse Transcription Kit (Applied Biosystems, Foster City, CA). Quantitative real-time PCR analysis was performed using SYBR Green in the real-time PCR system (Applied Biosystems, Warrington, UK). The thermal cycling program was 10 minutes at 95°C for enzyme activation and 40 cycles of denaturation for 15 seconds at 95°C, 30 seconds of annealing at 58°C, and 30 seconds of extension at 72°C. Primers used in the present study are listed in Table S1. The specificity of the PCR of genes was confirmed by one distinct band, which matched with the predicted size of the PCR amplicon (Figure S2). To normalize expression data, 18s rRNA was used as an internal control gene. Results are shown as relative expression of each target gene in SV-PVAT of each patient.

## Statistical Analysis

Numeric variables are expressed as means $\pm$ SEM for quantitative real-time PCR data, means $\pm$ SD for normal

distributions, and medians (interquartile ranges) for skewed variables. One-way repeated-measures ANOVA and paired *t*-test were used for detecting significant differences in data between SV-PVAT, ITA-PVAT, CA-PVAT, and Ao-PVAT, because a generalized linear mixed model analysis showed that there was no statistically significant interaction of any fat pad measure with age, sex, body mass index, or comorbidities, including diabetes mellitus, hypertension, dyslipidemia, and myocardial infarction, in the present study (data not shown).  $P < 0.05$  was considered statistically significant. All data were analyzed by using JMP15.2.1 for Macintosh (SAS Institute, Cary, NC).

## RESULTS

### Basal Characteristics of the Studied Patients

Basal characteristics of the 48 recruited patients (male/female, 32/16) who underwent elective CABG surgery using the SV are shown in Table 1. Age and body mass index of the recruited patients were  $72 \pm 8$  years and  $23.8 \pm 3.7$  kg/m<sup>2</sup>, respectively. The numbers of patients with current and former smoking habits were 7 (14.6%) and 31 (64.6%), respectively. Most of the patients (91.7%) were diagnosed with multivessel coronary artery disease. The numbers of patients with diabetes mellitus, hypertension, dyslipidemia, and myocardial infarction were 21 (43.8%), 39 (81.3%), 42 (87.5%), and 9 (18.6%), respectively. The ejection fraction assessed by echocardiography was  $55 \pm 12\%$ . Data for laboratory measurements are shown in Table 2.

### Adipocyte Sizes in Fat Pads

Representative hematoxylin-eosin staining of SV-PVAT, ITA-PVAT, CA-PVAT, and Ao-PVAT is shown in Figure 1A. Adipocyte size in SV-PVAT was significantly larger by 47%~57% than that in the other PVATs of vessels (Figure 1B). There was no significant difference in adipocyte size among ITA-PVAT, CA-PVAT, and Ao-PVAT. Crown-like structures, which have been reported to be composed of macrophages surrounding dead or dying adipocytes,<sup>27</sup> were observed in CA-PVAT and Ao-PVAT but not in SV-PVAT or ITA-PVAT.

### Fibrosis in Fat Pads

Representative Masson trichrome staining of PVAT is shown in Figure 2A. Samples for this fibrosis analysis were available from 28 of the 48 patients, and basal clinical characteristics in this subgroup of patients were similar to those in the entire study subjects (data not shown). The fibrosis areas in the inside, but not the edge, of adipose tissues were significantly larger in CA-PVAT and Ao-PVAT than in SV-PVAT and ITA-PVAT,

**Table 1. Characteristics of the Recruited Patients**

Characteristics	Values
No. (men/women)	48 (32/16)
Age, y	72±8
Body mass index	23.8±3.7
Waist circumference, cm	86.0±8.6
Systolic blood pressure, mm Hg	128±17
Diastolic blood pressure, mm Hg	67±15
Pulse rate, beats/min	70±9
Smoking habit, current/former/never	7 (14.6)/31 (64.6)/10 (20.8)
Drinking habit	18 (37.5)
Coronary artery disease	
1-Vessel disease	4 (8.3)
2-Vessel disease	15 (31.3)
3-Vessel disease	29 (60.4)
Complications	
Diabetes mellitus	21 (43.8)
Hypertension	39 (81.3)
Dyslipidemia	42 (87.5)
Myocardial infarction	9 (18.6)
Medications	
Oral antidiabetic drugs	16 (33.3)
Insulin	3 (6.3)
ACEI or ARB	21 (45.7)
β-Blocker	26 (54.2)
Statin	38 (79.2)
Antiplatelet drugs	38 (79.2)
Echocardiography	
Ejection fraction, %	55±12

Variables are expressed as number (percentage) or means±SD. ACEI indicates angiotensin-converting enzyme inhibitor; and ARB, angiotensin receptor blocker.

whereas the fibrosis area was significantly larger in Ao-PVAT than in CA-PVAT (Figure 2B). There was no significant difference in the fibrosis area between SV-PVAT and ITA-PVAT. CA-PVAT and Ao-PVAT had significantly higher gene expression levels of fibrosis-related molecules, transforming growth factor-β, tissue inhibitor of metalloproteinase 1, and macrophage-inducible C-type lectin, than did SV-PVAT and ITA-PVAT (Figure 2C). The gene expression level of another fibrosis-related molecule, platelet-derived growth factor subunit B, in CA-PVAT and that in Ao-PVAT were significantly higher than that in SV-PVAT (Figure 2C).

### Macrophage Infiltration in Fat Pads

Representative immunohistological staining, including CD68, a marker of macrophages, CD11c, a marker of M1 macrophages, and CD206, a marker of M2 macrophages, of PVAT is shown in Figure 3A. The macrophage infiltration area quantified by the

**Table 2. Laboratory Measurements**

Measures	Values
Hemoglobin, g/dL	11.5±2.0
AST, IU/L	26 (18–35)
ALT, IU/L	21 (13–36)
γGTP, IU/L	27 (17–40)
Blood urea nitrogen, mg/dL	17 (14–23)
Creatinine, mg/dL	0.96 (0.76–1.25)
eGFR, mL/min per 1.73 m <sup>2</sup>	54.5±19.3
Uric acid, mg/dL	5.6±1.6
Total cholesterol, mg/dL	141±45
LDL cholesterol, mg/dL	80±32
HDL cholesterol, mg/dL	42±11
Triglycerides, mg/dL	95 (59–126)
Fasting glucose, mg/dL	106 (93–129)
Insulin, μU/mL	5.1 (2.7–8.7)
HOMA-R	1.22 (0.62–3.15)
HbA1c, %	6.1±1.1
hs-CRP, mg/dL	0.14 (0.06–0.31)
NT-proBNP, pg/mL	288 (104–1004)

Variables are expressed as means±SD or medians (interquartile ranges). ALT indicates alanine transaminase; AST, aspartate transaminase; eGFR, estimated glomerular filtration rate; γGTP, γ-glutamyl transpeptidase; HbA1c, hemoglobin A1c; HDL, high-density lipoprotein; HOMA-R, homeostasis model assessment of insulin resistance; hs-CRP, high-sensitivity C-reactive protein; LDL, low-density lipoprotein; and NT-proBNP, N-terminal pro-B-type natriuretic peptide.

anti-CD68 antibody was significantly larger in CA-PVAT and Ao-PVAT than in SV-PVAT and ITA-PVAT, and there was no significant difference in the macrophage infiltration area between SV-PVAT and ITA-PVAT (Figure 3B). The inflammatory area of the M1 phenotype of macrophage infiltration quantified by the anti-CD11c antibody was significantly larger in CA-PVAT and Ao-PVAT than in SV-PVAT, and the area in CA-PVAT was larger than the areas in ITA-PVAT and Ao-PVAT (Figure 3C). The area of the M2 phenotype of macrophage infiltration quantified by the anti-CD206 antibody was significantly larger in CA-PVAT and Ao-PVAT than in SV-PVAT and ITA-PVAT (Figure 3D). The ratio of CD11c-positive/CD206-positive macrophages was significantly higher in CA-PVAT than in the other PVATs of vessels (Figure 3E).

### Metaflammation in Fat Pads

Gene expression levels of CD68, a marker of macrophages, CD11c, a marker of M1 macrophages, CD163 and CD206, M2 macrophage markers, and interleukin-10, an anti-inflammatory cytokine as an M2 macrophage-related marker, in CA-PVAT and those in Ao-PVAT were significantly higher than those in SV-PVAT (Figure 4A). Gene expression levels of CD68 and CD11c in CA-PVAT were significantly

higher than those in ITA-PVAT (Figure 4A). Gene expression levels of CD163, CD206, and interleukin-10 in ITA-PVAT were significantly higher than those in SV-PVAT (Figure 4A).

The gene expression level of adiponectin, an adipokine with antiatherogenic and anti-inflammatory features, in SV-PVAT was significantly higher than that in the other PVATs of vessels (Figure 4B). Gene expression levels of MCP-1 (monocyte chemoattractant protein-1), a chemokine, and inflammatory cytokines, including interleukin-1β and interleukin-6, were significantly higher in CA-PVAT and Ao-PVAT than in SV-PVAT and ITA-PVAT (Figure 4B). The gene expression level of tumor necrosis factor-α, an inflammatory cytokine, in SV-PVAT was significantly lower than that in the other PVATs of vessels (Figure 4B).

Gene expression levels of inflammasome-related molecules, including nucleotide-binding domain, leucine-rich-containing family, pyrin domain-containing-3 and ASC (apoptosis-associated speck-like protein containing caspase recruitment domain), and endoplasmic reticulum stress-related molecules, including GRP78 (glucose-regulated protein 78) and CHOP (C/EBP homologous protein), were significantly higher in CA-PVAT and Ao-PVAT than in SV-PVAT (Figure 4C). Gene expression levels of nucleotide-binding domain, leucine-rich-containing family, pyrin domain-containing-3, GRP78, and CHOP in CA-PVAT were significantly higher than those in ITA-PVAT (Figure 4C).

### Adipocyte Developmental and Pattern-Forming Genes in Fat Pads

To further address phenotypic differences between adipose tissues in the 4 perivascular parts, we examined gene expression levels of adipocyte developmental and pattern-forming genes, including engrailed homeobox 1, empty spiracles homeobox 2, and homeobox A5, as in previous studies.<sup>15,28–30</sup> The gene expression level of engrailed homeobox 1 was significantly higher in SV-PVAT than in the other PVATs of vessels (Figure 5A). The expression level of empty spiracles homeobox 2 was significantly higher in SV-PVAT than in the other PVATs, and the empty spiracles homeobox 2 level in CA-PVAT was significantly higher than the levels in ITA-PVAT and Ao-PVAT (Figure 5B). The gene expression level of homeobox A5 was significantly higher in ITA-PVAT than in the other PVATs, and the homeobox A5 level in SV-PVAT was significantly higher than the levels in CA-PVAT and Ao-PVAT (Figure 5C).

## DISCUSSION

To the best of our knowledge, the present study is the first study to demonstrate a differential phenotype of metaflammation in fat pads surrounding the SV in

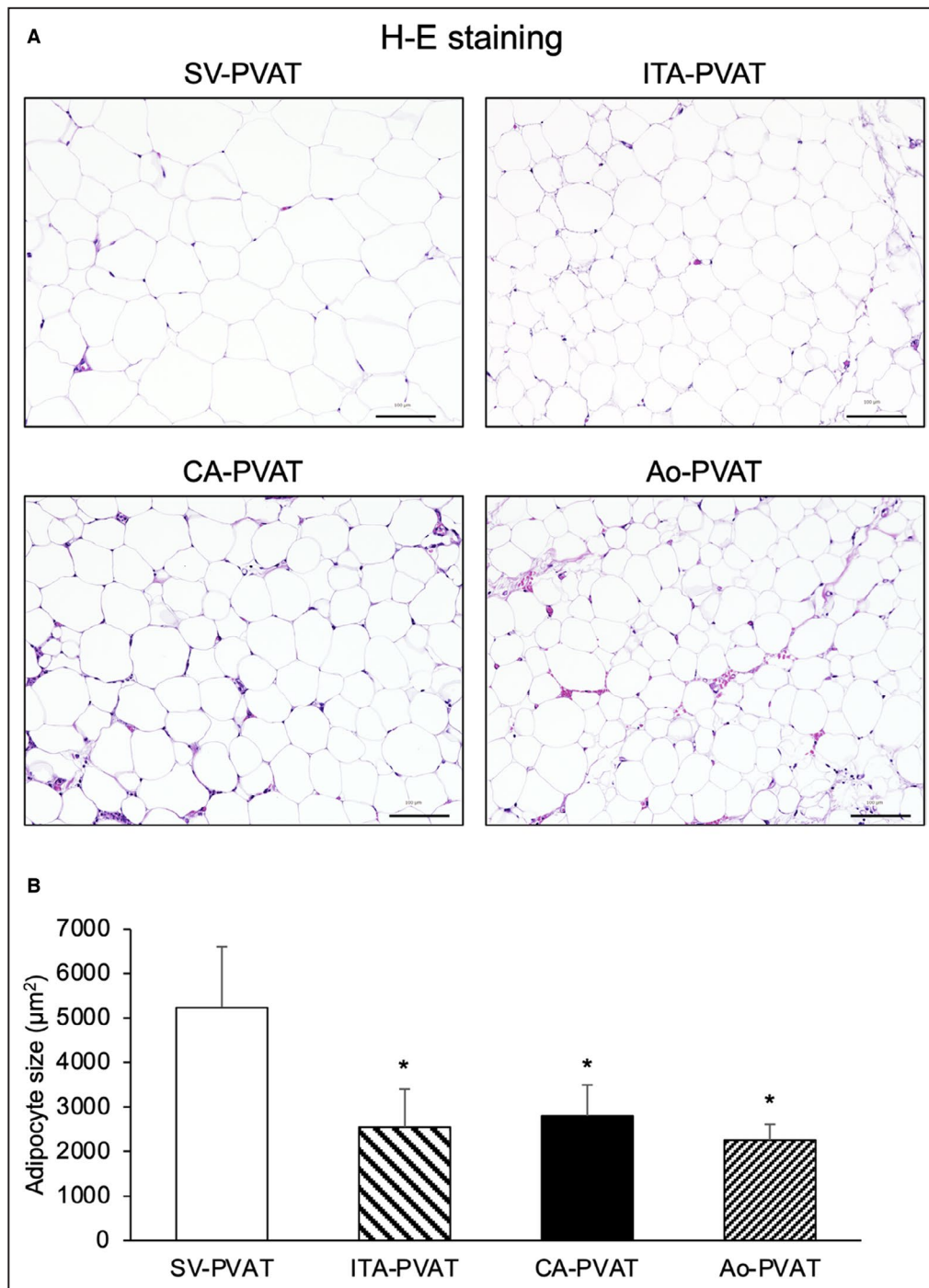


**Figure 1. Adipocyte sizes in fat pads.**

**A**, Representative hematoxylin-eosin (H-E) staining of perivascular adipose tissue surrounding the saphenous vein (SV-PVAT), that surrounding the internal thoracic artery (ITA-PVAT), that surrounding the coronary artery (CA-PVAT), and that surrounding the aorta (Ao-PVAT). Bar=100 µm. **B**, Comparison of adipocyte sizes in SV-PVAT, ITA-PVAT, CA-PVAT, and Ao-PVAT of patients (n=48). Results are shown as means±SD. \* $P<0.05$  vs SV-PVAT.

direct comparison to fat pads surrounding the coronary artery, ITA, and aorta. Interestingly, SV-PVAT was shown to have lower levels of metaflammation and consecutive adipose tissue remodeling (namely,

augmented immune cell infiltration, induction of inflammatory cytokines, activation of inflammasomes and endoplasmic reticulum stress, and increased fibrosis) than those in CA-PVAT and Ao-PVAT. The

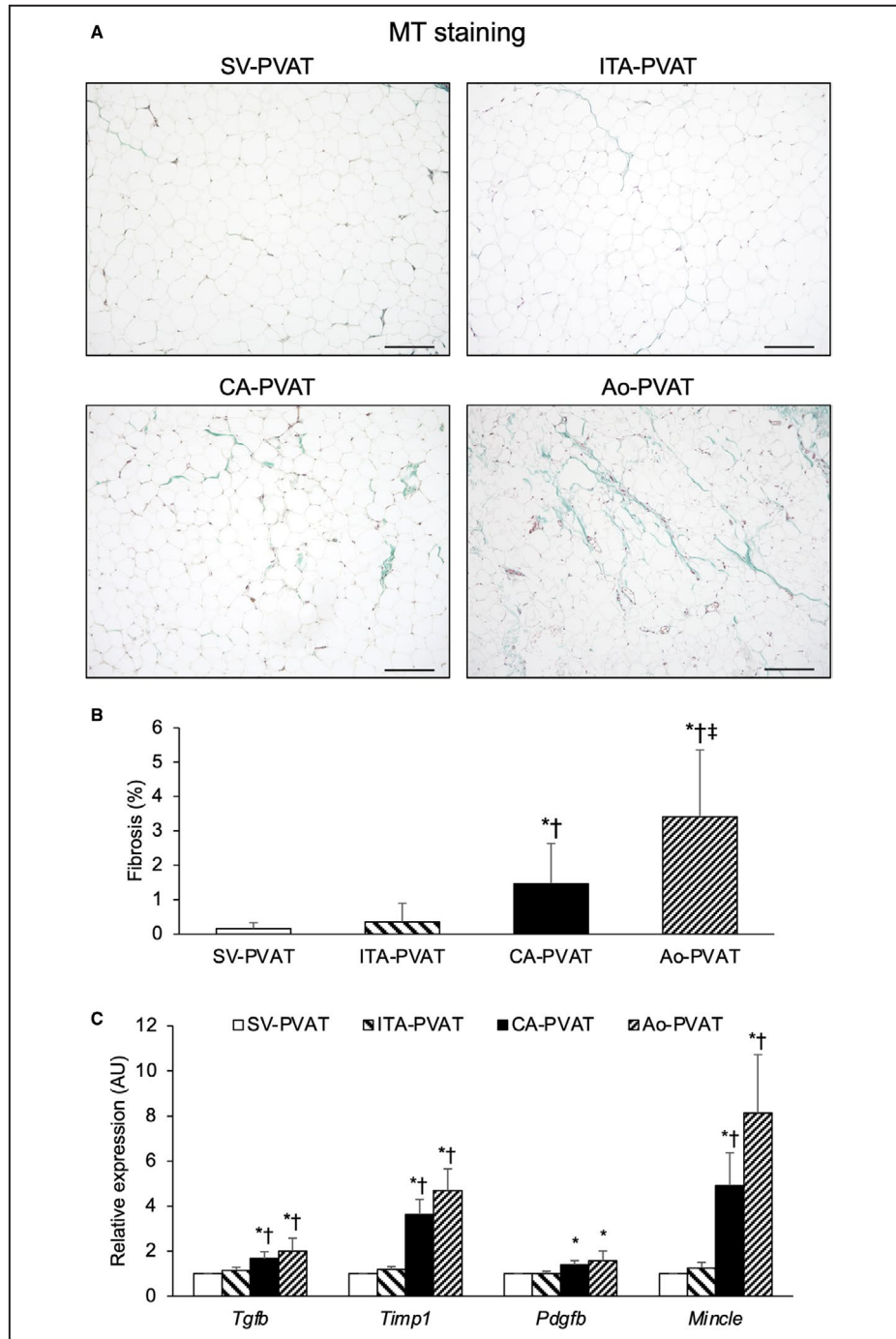


**Figure 2. Fibrosis in fat pads.**

**A**, Representative Masson trichrome (MT) staining of perivascular adipose tissue surrounding the saphenous vein (SV-PVAT), that surrounding the internal thoracic artery (ITA-PVAT), that surrounding the coronary artery (CA-PVAT), and that surrounding the aorta (Ao-PVAT). Bar=200  $\mu$ m. **B**, Fibrosis areas in SV-PVAT, ITA-PVAT, CA-PVAT, and Ao-PVAT of patients (n=28). Results are shown as means $\pm$ SD. **C**, Gene expression levels of fibrosis-related molecules, including transforming growth factor- $\beta$  (TGF- $\beta$ ), tissue inhibitor of metalloproteinase 1 (TIMP1), platelet-derived growth factor subunit B (PDGFB), and macrophage-inducible C-type lectin (MINCLE), in SV-PVAT, ITA-PVAT, CA-PVAT, and Ao-PVAT. Results are shown as relative expression of each target gene in SV-PVAT of each patient (n=48) and as means $\pm$ SEM for quantitative real-time polymerase chain reaction data. AU indicates arbitrary unit. \* $P$ <0.05 vs SV-PVAT, † $P$ <0.05 vs ITA-PVAT, ‡ $P$ <0.05 vs CA-PVAT.

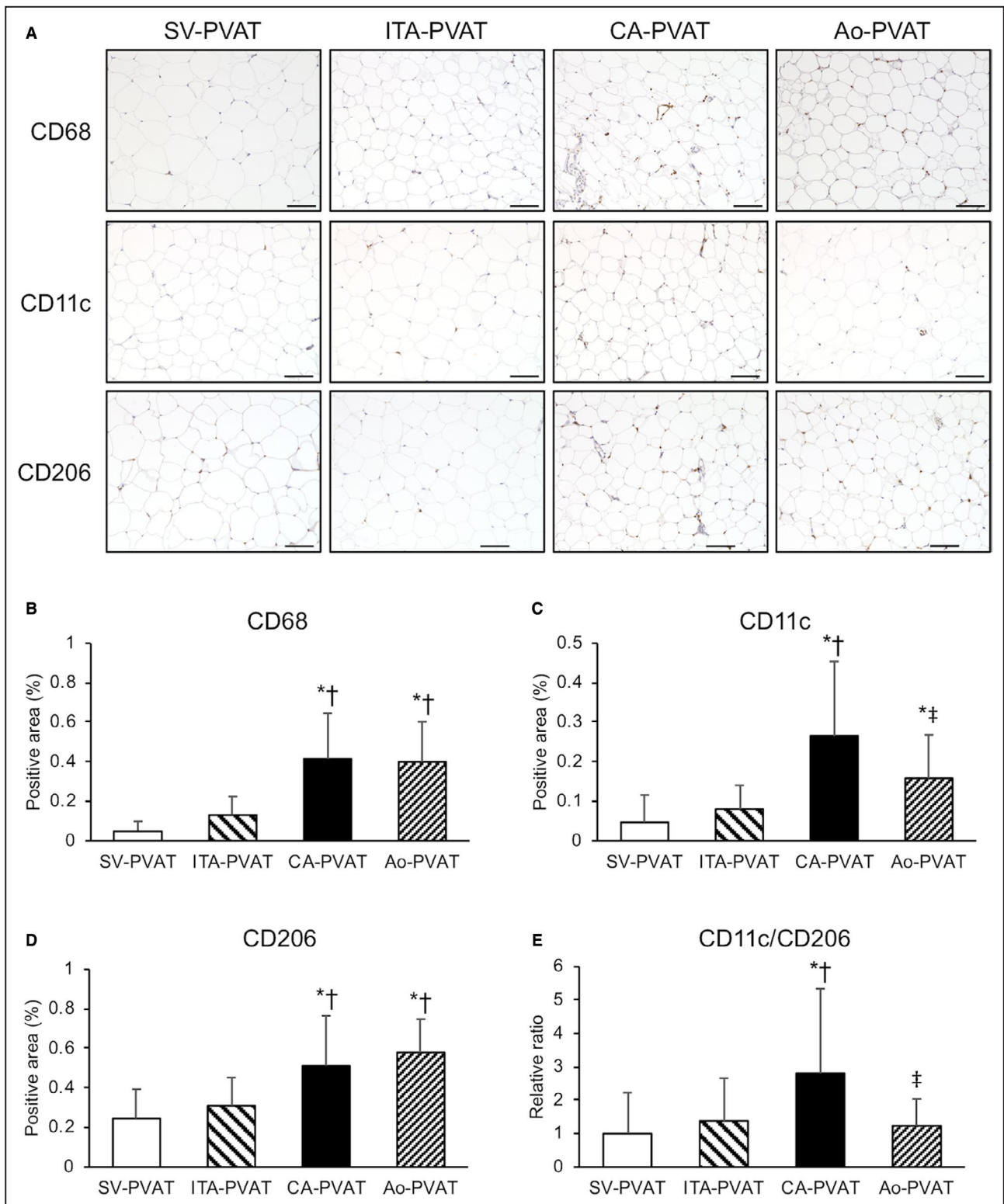
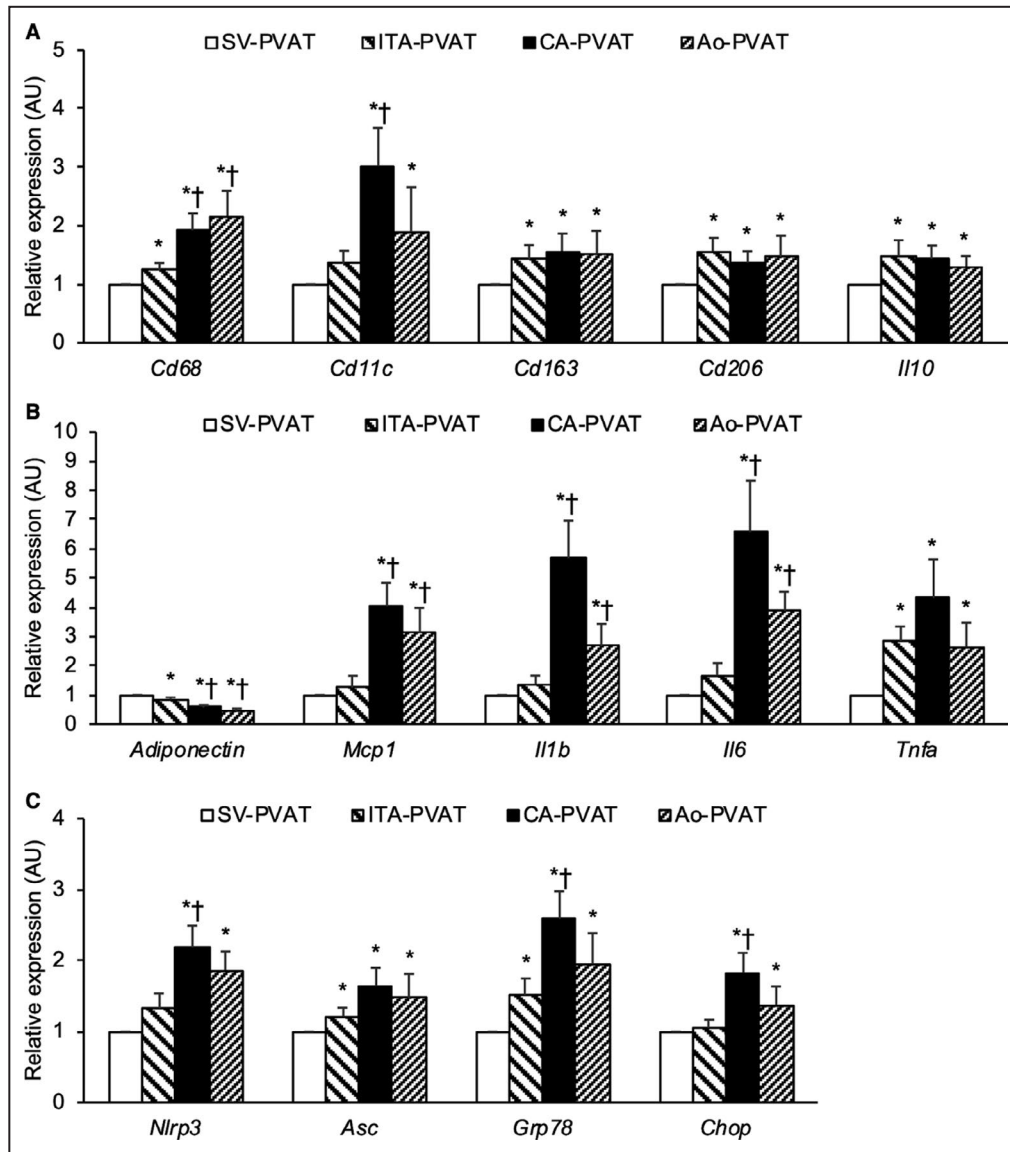


**Figure 3. Macrophage infiltration in fat pads.** **A**, Representative immunohistological staining, including cluster of differentiation (CD) 68 (a marker of macrophages), CD11c (a marker of M1 macrophages), and CD206 (a marker of M2 macrophages), of perivascular adipose tissue surrounding the saphenous vein (SV-PVAT), that surrounding the internal thoracic artery (ITA-PVAT), that surrounding the coronary artery (CA-PVAT), and that surrounding the aorta (Ao-PVAT). Bar=100  $\mu$ m. **B** through **D**, Positive areas of immunohistological staining of CD68, CD11c, and CD206 in SV-PVAT, ITA-PVAT, CA-PVAT, and Ao-PVAT of patients (n=28). **E**, Ratios of the macrophage infiltration areas of CD11c/CD206 in SV-PVAT, ITA-PVAT, CA-PVAT, and Ao-PVAT. Results are shown as means $\pm$ SD. \* $P$ <0.05 vs SV-PVAT, † $P$ <0.05 vs ITA-PVAT, ‡ $P$ <0.05 vs CA-PVAT.





level of metaflammation was higher in CA-PVAT than in Ao-PVAT, as indicated by a significantly larger extent of CD11c-positive M1 macrophage infiltration, and higher ratio of CD11c-positive M1/CD206-positive M2 macrophages. The phenotype

of SV-PVAT was closer to that of ITA-PVAT than the other PVATs. We previously reported that ITA-PVAT had less metaflammation, which may be related to the decreased atherosclerosis in the ITA used as the gold standard graft material in CABG.<sup>15</sup>

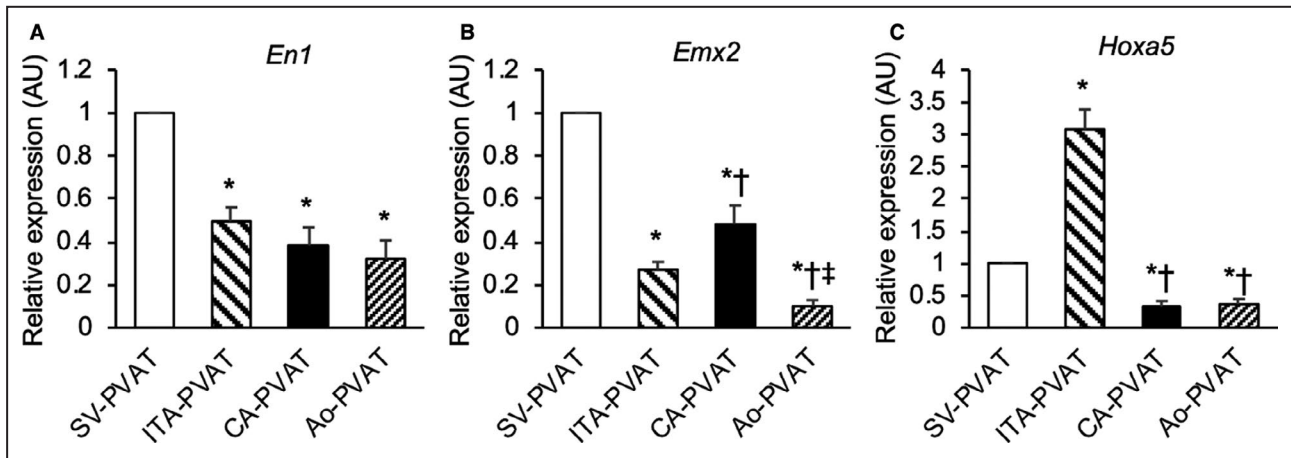


**Figure 5. Adipocyte developmental and pattern-forming factors in fat pads.**

**A** through **C**, Gene expression levels of adipocyte developmental and pattern-forming factors, including engrailed homeobox 1 (EN1) (**A**), empty spiracles homeobox 2 (EMX2) (**B**), and homeobox A5 (HOXA5) (**C**), in perivascular adipose tissue surrounding the saphenous vein (SV-PVAT), that surrounding the internal thoracic artery (ITA-PVAT), that surrounding the coronary artery (CA-PVAT), and that surrounding the aorta (Ao-PVAT). Results are shown as relative expression of each target gene in SV-PVAT of each patient (n=48) and as means±SEM for quantitative real-time polymerase chain reaction data. AU indicates arbitrary unit. \* $P<0.05$  vs SV-PVAT, † $P<0.05$  vs ITA-PVAT, ‡ $P<0.05$  vs CA-PVAT.

The conventional SV harvesting removes all the vasa vasorum, resulting in ischemia of the wall in the SV.<sup>13</sup> Physical damage of the endothelial layer also occurs during the preparation of a graft by high-pressure dilation of the vein, and degenerative and atherosclerotic processes can be promoted when a venous graft is implanted in the arterial circulation.<sup>13</sup> In contrast, in the “no-touch” technique, the SV is harvested together with its surrounding tissues.<sup>16</sup> The use of this novel technique has been reported to result in better short- and long-term graft patency rates than those achieved by using the conventional technique of SV harvesting, and the rates were comparable to those for ITA grafts.<sup>17–19</sup> Several mechanisms underlying the clinical benefit (or advantage) of no-touch vein grafts have been proposed. In the no-touch vein pedicle, the perivascular tissue is preserved and acts as a natural, external, and biological stent that consists of numerous collagen fibers, leading to prevention of the deleterious effects of aortic pressure to the vein wall and reduction of early thrombotic occlusion, neointimal and medial thickening, and kinking of the vein graft.<sup>17–19</sup> In addition, preservation of the vasa vasorum allows retrograde blood flow from the graft lumen to perfuse through the vein wall, leading to a decrease in transmural ischemic damage.<sup>31</sup> Furthermore, endothelial NO synthase is preserved in all 3 layers of the vein wall after the no-touch technique,<sup>31,32</sup> whereas stripping and distention used during the conventional technique lead to a reduction of endothelial NO synthase.<sup>32,33</sup> It has also been proposed that SV-PVAT can be a source of several vasoactive factors.<sup>23,24</sup> In the present study, we

demonstrated that SV-PVAT had an antiatherosclerotic phenotype, such as less metaflammation and proinflammatory cytokines. In addition, we found that such a phenotype of SV-PVAT is similar to that of ITA-PVAT. Taken together, the findings of the present study suggest that distinct phenotype of SV-PVAT is linked to a high rate of long-term patency of grafting in CABG using the no-touch technique of SV harvesting.

Anatomically separated regional fat pads have distinct gene expression patterns and functional characteristics.<sup>28–30</sup> It has been reported that in vitro differentiation of preadipocytes isolated from regional adipose depots produces adipocytes that phenotypically resemble in vivo counterparts of adipocytes.<sup>28–30,34</sup> Phenotypic differences in adipocytes can stem from developmental divergence of precursor cells in distinct adipose tissue. In the present study, the expression patterns of adipocyte developmental and pattern-forming genes,<sup>15,28–30</sup> including engrailed homeobox 1, empty spiracles homeobox 2, and homeobox A5, were totally different among SV-PVAT, ITA-PVAT, CA-PVAT, and Ao-PVAT. These findings are consistent with the notion that adipocytes residing in these depots are derived from distinct precursor cells, which may underlie the phenotypic differences, although immune cells in adipose tissue may have some acquired effects.

The physiological development of PVAT has been reported to be reduced and impaired with increased inflammation in experimental models of atherosclerosis and endovascular injury.<sup>35–37</sup> Conversely, removal of normally functioning PVAT or implantation of PVAT

with a proinflammatory phenotype promoted atherosclerosis, suggesting that the lack of normal PVAT is sufficient to drive increased atherosclerosis.<sup>38</sup> Autopsy analyses demonstrated that there was more macrophage infiltration in epicardial fat in vessels with large necrotic core plaques than in vessels without lipid core plaques.<sup>39,40</sup> In the present study, patients without coronary artery disease were not included as a control group. Therefore, it is difficult to determine whether the inflammatory response in PVAT is the cause or the result of atherosclerosis. Mechanistic studies are needed to clarify what underlies the relationship between the development of atherosclerosis and differential phenotypes of PVAT.

This study has several limitations. First, the number of patients was small, and there would have been selection bias of patients. However, the clinical profile of the patients enrolled in this study was not deviated from the average profiles in patients registered in Japan Cardiovascular Surgery Database. Second, because the recruited patients were only Japanese people, it is unclear whether the present findings can be generalized to other ethnicities. Third, because this study was a cross-sectional study using patients with coronary artery disease, the study does not prove a causal relationship between inflammatory changes in adipose tissue and the development and progression of atherosclerosis in the vein grafts. Interventional studies of CABG using the conventional technique as a control and the no-touch technique of SV harvesting are necessary for investigating the relationship between inflammatory changes in adipose tissue and graft patency in the future. Fourth, the recruited patients had several diseases, including diabetes mellitus, hypertension, and dyslipidemia, and had been treated with several drugs, including angiotensin-converting enzyme inhibitors, angiotensin receptor blockers, and statins. Pretreatment with several drugs may have affected the extent of metaflammation and fibrosis in adipose tissue. Fifth, most of the recruited patients in the present study were adequately treated and were not obese, and risk factors in patients had been controlled well at the time of the operation of CABG. Such conditions may have affected the extent of inflammation and remodeling in adipose tissue. Finally, the gene expression of molecules was mainly investigated because of the small amount of fat pads in the present study, but the protein expression of molecules needs to be investigated in the future.

In conclusion, SV-PVAT has a distinct histological and gene expression phenotype, resulting from inherent differences in adipocytes, and is protected from metaflammation and consecutive adipose tissue remodeling in patients who have undergone elective CABG surgery. There are similarities in the gene

expression phenotypes of SV-PVAT and PVAT surrounding the ITA, an atherosclerosis-resistant vessel. The phenotype of SV-PVAT might be linked to the high rate of long-term patency of grafting in CABG using the no-touch technique of SV harvesting.

## ARTICLE INFORMATION

Received August 10, 2020; accepted February 22, 2021.

### Affiliations

From the Department of Cardiovascular Surgery (T.M., R.N., R.H., S.N., T.K., N.K.) and Department of Cardiovascular, Renal and Metabolic Medicine (M.F., A.S., Y.H., M.T., T.M.), Sapporo Medical University School of Medicine, Sapporo, Japan; Department of Cardiovascular Surgery, Hokkaido Ohno Memorial Hospital, Sapporo, Japan (S.O.); Department of Cardiovascular Surgery, Sapporo Central Hospital, Sapporo, Japan (T.S.); Department of Cardiovascular Surgery, Sapporo City General Hospital, Sapporo, Japan (M.N.); Department of Cardiovascular Surgery, Teine Keijinkai Hospital, Sapporo, Japan (Y.I.); and Department of Cardiovascular Surgery, Otaru City General Hospital, Otaru, Japan (J.F.).

### Sources of Funding

Dr Furuhashi has been supported by a grant from Japan Society for the Promotion of Science.

### Disclosures

None.

### Supplementary Material

Table S1

Figures S1–S2

## REFERENCES

1. Szasz T, Webb RC. Perivascular adipose tissue: more than just structural support. *Clin Sci (Lond)*. 2012;122:1–12. DOI: 10.1042/CS20110151.
2. Mendizabal Y, Llorens S, Nava E. Vasoactive effects of prostaglandins from the perivascular fat of mesenteric resistance arteries in WKY and SHROB rats. *Life Sci*. 2013;93:1023–1032. DOI: 10.1016/j.lfs.2013.10.021.
3. Meyer MR, Fredette NC, Barton M, Prossnitz ER. Regulation of vascular smooth muscle tone by adipose-derived contracting factor. *PLoS One*. 2013;8:e79245. DOI: 10.1371/journal.pone.0079245.
4. Owen MK, Witzmann FA, McKenney ML, Lai X, Berwick ZC, Moberly SP, Alloosh M, Sturek M, Tune JD. Perivascular adipose tissue potentiates contraction of coronary vascular smooth muscle: influence of obesity. *Circulation*. 2013;128:9–18. DOI: 10.1161/CIRCULATIONAHA.112.001238.
5. Saxton SN, Ryding KE, Aldous RG, Withers SB, Ohanian J, Heagerty AM. Role of sympathetic nerves and adipocyte catecholamine uptake in the vasorelaxant function of perivascular adipose tissue. *Arterioscler Thromb Vasc Biol*. 2018;38:880–891. DOI: 10.1161/ATVBAHA.118.310777.
6. Mazurek T, Zhang L, Zalewski A, Mannion JD, Diehl JT, Arafat H, Sarov-Blat L, O'Brien S, Keiper EA, Johnson AG, et al. Human epicardial adipose tissue is a source of inflammatory mediators. *Circulation*. 2003;108:2460–2466. DOI: 10.1161/01.CIR.0000099542.57313.C5.
7. Greif M, Becker A, von Ziegler F, Lebherz C, Lehrke M, Broedel UC, Tittus J, Parhofer K, Becker C, Reiser M, et al. Pericardial adipose tissue determined by dual source CT is a risk factor for coronary atherosclerosis. *Arterioscler Thromb Vasc Biol*. 2009;29:781–786. DOI: 10.1161/ATVBAHA.108.180653.
8. Shimabukuro M, Hirata Y, Tabata M, Dagvasumberel M, Sato H, Kurobe H, Fukuda D, Soeki T, Kitagawa T, Takanashi S, et al. Epicardial adipose tissue volume and adipocytokine imbalance are strongly linked to human coronary atherosclerosis. *Arterioscler Thromb Vasc Biol*. 2013;33:1077–1084. DOI: 10.1161/ATVBAHA.112.300829.

9. Furuhashi M, Fuseya T, Murata M, Hoshina K, Ishimura S, Mita T, Watanabe Y, Omori A, Matsumoto M, Sugaya T, et al. Local production of fatty acid-binding protein 4 in epicardial/perivascular fat and macrophages is linked to coronary atherosclerosis. *Arterioscler Thromb Vasc Biol.* 2016;36:825–834. DOI: 10.1161/ATVBAHA.116.307225.
10. Ohyama K, Matsumoto Y, Takanami K, Ota H, Nishimiya K, Sugisawa J, Tsuchiya S, Amamizu H, Uzuka H, Suda A, et al. Coronary adventitial and perivascular adipose tissue inflammation in patients with vasospastic angina. *J Am Coll Cardiol.* 2018;71:414–425. DOI: 10.1016/j.jacc.2017.11.046.
11. Hotamisligil GS. Inflammation, metaflammation and immunometabolic disorders. *Nature.* 2017;542:177–185. DOI: 10.1038/nature21363.
12. Otsuka F, Yahagi K, Sakakura K, Virmani R. Why is the mammary artery so special and what protects it from atherosclerosis? *Ann Cardiothorac Surg.* 2013;2:519–526. DOI: 10.3978/j.issn.2225-319X.2013.07.06.
13. Kitamura S. Physiological and metabolic effects of grafts in coronary artery bypass surgery. *Circ J.* 2011;75:766–772. DOI: 10.1253/circj.CJ-10-1302.
14. Nakajima T, Tachibana K, Takagi N, Ito T, Kawaharada N. Histomorphologic superiority of internal thoracic arteries over right gastroepiploic arteries for coronary bypass. *J Thorac Cardiovasc Surg.* 2016;151:1704–1708. DOI: 10.1016/j.jtcvs.2016.02.018.
15. Numaguchi R, Furuhashi M, Matsumoto M, Sato H, Yanase Y, Kuroda Y, Harada R, Ito T, Higashiura Y, Koyama M, et al. Differential phenotypes in perivascular adipose tissue surrounding the internal thoracic artery and diseased coronary artery. *J Am Heart Assoc.* 2019;8:e011147. DOI: 10.1161/JAHA.118.011147.
16. Souza D. A new no-touch preparation technique: technical notes. *Scand J Thorac Cardiovasc Surg.* 1996;30:41–44. DOI: 10.3109/14017439609107239.
17. Souza DS, Johansson B, Bojo L, Karlsson R, Geijer H, Filbey D, Bodin L, Arbeus M, Dashwood MR. Harvesting the saphenous vein with surrounding tissue for CABG provides long-term graft patency comparable to the left internal thoracic artery: results of a randomized longitudinal trial. *J Thorac Cardiovasc Surg.* 2006;132:373–378. DOI: 10.1016/j.jtcvs.2006.04.002.
18. Sepehrpour AH, Jarral OA, Shipolini AR, McCormack DJ. Does a “no-touch” technique result in better vein patency? *Interact Cardiovasc Thorac Surg.* 2011;13:626–630. DOI: 10.1510/icvts.2011.281998.
19. Papakonstantinou NA, Baikoussis NG, Goudevenos J, Papadopoulos G, Apostolakis E. Novel no touch technique of saphenous vein harvesting: is great graft patency rate provided? *Ann Card Anaesth.* 2016;19:481–488. DOI: 10.4103/0971-9784.185537.
20. Dreifaldt M, Souza DS, Loesch A, Muddle JR, Karlsson MG, Filbey D, Bodin L, Norgren L, Dashwood MR. The “no-touch” harvesting technique for vein grafts in coronary artery bypass surgery preserves an intact vasa vasorum. *J Thorac Cardiovasc Surg.* 2011;141:145–150. DOI: 10.1016/j.jtcvs.2010.02.005.
21. Souza DS, Christofferson RH, Bomfim V, Filbey D. “No-touch” technique using saphenous vein harvested with its surrounding tissue for coronary artery bypass grafting maintains an intact endothelium. *Scand Cardiovasc J.* 1999;33:323–329. DOI: 10.1080/14017439950141362.
22. Tsui JC, Souza DS, Filbey D, Bomfim V, Dashwood MR. Preserved endothelial integrity and nitric oxide synthase in saphenous vein grafts harvested by a “no-touch” technique. *Br J Surg.* 2001;88:1209–1215. DOI: 10.1046/j.0007-1323.2001.01855.x.
23. Gollasch M, Dubrovskaja G. Paracrine role for periadventitial adipose tissue in the regulation of arterial tone. *Trends Pharmacol Sci.* 2004;25:647–653. DOI: 10.1016/j.tips.2004.10.005.
24. Dashwood MR, Dooley A, Shi-Wen X, Abraham DJ, Dreifaldt M, Souza DS. Perivascular fat-derived leptin: a potential role in improved vein graft performance in coronary artery bypass surgery. *Interact Cardiovasc Thorac Surg.* 2011;12:170–173. DOI: 10.1510/icvts.2010.247874.
25. Ishimura S, Furuhashi M, Mita T, Fuseya T, Watanabe Y, Hoshina K, Kokubu N, Inoue K, Yoshida H, Miura T. Reduction of endoplasmic reticulum stress inhibits neointima formation after vascular injury. *Sci Rep.* 2014;4:6943. DOI: 10.1038/srep06943.
26. Koyama M, Furuhashi M, Ishimura S, Mita T, Fuseya T, Okazaki Y, Yoshida H, Tsuchihashi K, Miura T. Reduction of endoplasmic reticulum stress by 4-phenylbutyric acid prevents the development of hypoxia-induced pulmonary arterial hypertension. *Am J Physiol Heart Circ Physiol.* 2014;306:H1314–H1323. DOI: 10.1152/ajpheart.00869.2013.
27. Cinti S, Mitchell G, Barbatelli G, Murano I, Ceresi E, Faloia E, Wang S, Fortier M, Greenberg AS, Obin MS. Adipocyte death defines macrophage localization and function in adipose tissue of obese mice and humans. *J Lipid Res.* 2005;46:2347–2355. DOI: 10.1194/jlr.M500294-JLR200.
28. Gesta S, Blüher M, Yamamoto Y, Norris AW, Berndt J, Kralisch S, Boucher J, Lewis C, Kahn CR. Evidence for a role of developmental genes in the origin of obesity and body fat distribution. *Proc Natl Acad Sci USA.* 2006;103:6676–6681. DOI: 10.1073/pnas.0601752103.
29. Tchkonina T, Lenburg M, Thomou T, Giordano N, Frampton G, Pirtskhalava T, Cartwright A, Cartwright M, Flanagan J, Karagiannides I, et al. Identification of depot-specific human fat cell progenitors through distinct expression profiles and developmental gene patterns. *Am J Physiol Endocrinol Metab.* 2007;292:E298–E307. DOI: 10.1152/ajpen.00202.2006.
30. Chatterjee TK, Stoll LL, Denning GM, Harrelson A, Blomkalns AL, Idelman G, Rothenberg FG, Neltner B, Romig-Martin SA, Dickson EW, et al. Proinflammatory phenotype of perivascular adipocytes: influence of high-fat feeding. *Circ Res.* 2009;104:541–549. DOI: 10.1161/CIRCRESAHA.108.182998.
31. Dreifaldt M, Souza D, Bodin L, Shi-Wen X, Dooley A, Muddle J, Loesch A, Dashwood MR. The vasa vasorum and associated endothelial nitric oxide synthase is more important for saphenous vein than arterial bypass grafts. *Angiology.* 2013;64:293–299. DOI: 10.1177/0003319712443729.
32. Dashwood MR, Savage K, Dooley A, Shi-Wen X, Abraham DJ, Souza DS. Effect of vein graft harvesting on endothelial nitric oxide synthase and nitric oxide production. *Ann Thorac Surg.* 2005;80:939–944. DOI: 10.1016/j.athoracsur.2005.03.042.
33. Rueda F, Souza D, Lima Rde C, Menezes A, Johansson B, Dashwood M, The E, Gesteira M, Escobar M, Vasconcelos F. Novel no-touch technique of harvesting the saphenous vein for coronary artery bypass grafting. *Arq Bras Cardiol.* 2008;90:356–362. DOI: 10.1590/s0066-782x2008000600002.
34. Rittig K, Dolderer JH, Balletshofer B, Machann J, Schick F, Meile T, Küper M, Stock UA, Staiger H, Machicao F, et al. The secretion pattern of perivascular fat cells is different from that of subcutaneous and visceral fat cells. *Diabetologia.* 2012;55:1514–1525. DOI: 10.1007/s00125-012-2481-9.
35. Faight E, Verdellis K, Ahearn JM, Shields KJ. 3D microCT spatial and temporal characterization of thoracic aorta perivascular adipose tissue and plaque volumes in the ApoE<sup>-/-</sup> mouse model. *Adipocyte.* 2018;7:156–165. DOI: 10.1080/21623945.2018.1493900.
36. Xiong W, Zhao X, Villacorta L, Rom O, Garcia-Barrio MT, Guo Y, Fan Y, Zhu T, Zhang J, Zeng R, et al. Brown adipocyte-specific PPARγ (peroxisome proliferator-activated receptor gamma) deletion impairs perivascular adipose tissue development and enhances atherosclerosis in mice. *Arterioscler Thromb Vasc Biol.* 2018;38:1738–1747. DOI: 10.1161/ATVBAHA.118.311367.
37. Takaoka M, Suzuki H, Shioda S, Sekikawa K, Saito Y, Nagai R, Sata M. Endovascular injury induces rapid phenotypic changes in perivascular adipose tissue. *Arterioscler Thromb Vasc Biol.* 2010;30:1576–1582. DOI: 10.1161/ATVBAHA.110.207175.
38. Tanaka K, Sata M. Roles of perivascular adipose tissue in the pathogenesis of atherosclerosis. *Front Physiol.* 2018;9:3. DOI: 10.3389/fphys.2018.00003.
39. Sacks HS, Fain JN. Human epicardial adipose tissue: a review. *Am Heart J.* 2007;153:907–917. DOI: 10.1016/j.ahj.2007.03.019.
40. Vela D, Buja LM, Madjid M, Burke A, Naghavi M, Willerson JT, Casscells SW, Litovsky S. The role of periadventitial fat in atherosclerosis. *Arch Pathol Lab Med.* 2007;131:481–487. DOI: 10.5858/2007-131-481-TROFFI.

# **SUPPLEMENTAL MATERIAL**

**Table S1. Primers for human genes in quantitative real-time PCR.**

<i>Genes</i>	Accession #	Forward primer		Reverse primer		Amplicon size (bp)
<i>18s</i>	M10098	5'-GTAACCCGTTGAACCCATT	-3'	5'-CCATCCAATCGGTAGTAGCG	-3'	151
<i>Adiponectin</i>	NM_004797	5'-GTCATGACCAGGAAACCAC	-3'	5'-TTCACCGATGTCTCCCTTAGG	-3'	203
<i>Asc</i>	NM_145182	5'-TGGATGCTCTGTACGGGAAG	-3'	5'-CCAGGCTGGTGTGAAACTGAA	-3'	110
<i>Cd11c</i>	NM_000887	5'-CTGCAAGGGTTTACATACACGG	-3'	5'-GAATTTTGGCGGCATCCCTAC	-3'	97
<i>Cd68</i>	NM_001040059	5'-CTTCTCTCATTCCCCTATGGACA	-3'	5'-GAAGGACACATTGACTCCACC	-3'	105
<i>Cd163</i>	NM_004244	5'-GCGGGAGAGTGGAAGTGAAAG	-3'	5'-GTTACAAATCACAGAGACCGCT	-3'	89
<i>Cd206</i>	NM_002438	5'-GGGTTGCTATCACTCTCTATGC	-3'	5'-TTTCTTGCTGTTGCCGTAGTT	-3'	126
<i>Chop</i>	NM_004083	5'-GGAGAACCAGGAAACGGAAAC	-3'	5'-TCTCCTTCATGCGCTGCTTT	-3'	69
<i>Emx2</i>	NM_004098	5'-CGGCACTCAGCTACGCTAAC	-3'	5'-CAAGTCCGGGTTGGAGTAGAC	-3'	107
<i>En1</i>	NM_001426	5'-GAGCGCAGGGCACCAAATA	-3'	5'-CGAGTCAGTTTTGACCACGG	-3'	92
<i>Grp78</i>	NM_005347	5'-CATCACGCCGTCCTATGTCG	-3'	5'-CGTCAAAGACCGTGTTCTCG	-3'	104
<i>Hoxa5</i>	NM_019102	5'-AACTCATTTTGCGGTCGCTAT	-3'	5'-TCCCTGAATTGCTCGCTCAC	-3'	89
<i>Il1b</i>	NM_000576	5'-CACGATGCACCTGTACGATCA	-3'	5'-GTTGCTCCATATCCTGTCCCT	-3'	121
<i>Il6</i>	NM_000600	5'-AAATTCGGTACATCCTCGACGG	-3'	5'-GGAAGGTTTCAGGTTGTTTTCTGC	-3'	112
<i>Il10</i>	NM_000572	5'-GACTTTAAGGGTTACCTGGGTTG	-3'	5'-TCACATGCGCCTTGATGTCTG	-3'	112
<i>Mcp1</i>	NM_002982	5'-CAGCCAGATGCAATCAATGCC	-3'	5'-TGGAATCCTGAACCCACTTCT	-3'	190
<i>Mincle</i>	NM_014358	5'-CTGAAACACAATGCACAGAGAGA	-3'	5'-AAAGATGCGAAATGTCACAACAC	-3'	128
<i>Nlrp3</i>	NM_001127462	5'-GATCTTCGCTGCGATCAACAG	-3'	5'-CGTGCATTATCTGAACCCAC	-3'	81
<i>Pdgfb</i>	NM_033016.2	5'-CTCGATCCGCTCCTTTGATGA	-3'	5'-CGTTGGTGCGGTCTATGAG	-3'	239
<i>Tgfb</i>	NM_000660	5'-CAAGCAGAGTACACACAGCAT	-3'	5'-TGCTCCACTTTTAACTTGAGCC	-3'	126
<i>Timp1</i>	NM_003254	5'-CTTCTGCAATTCCGACCTCGT	-3'	5'-ACGCTGGTATAAGGTGGTCTG	-3'	79
<i>Tnfa</i>	NM_000594	5'-GAGGCCAAGCCCTGGTATG	-3'	5'-CGGGCCGATTGATCTCAGC	-3'	91

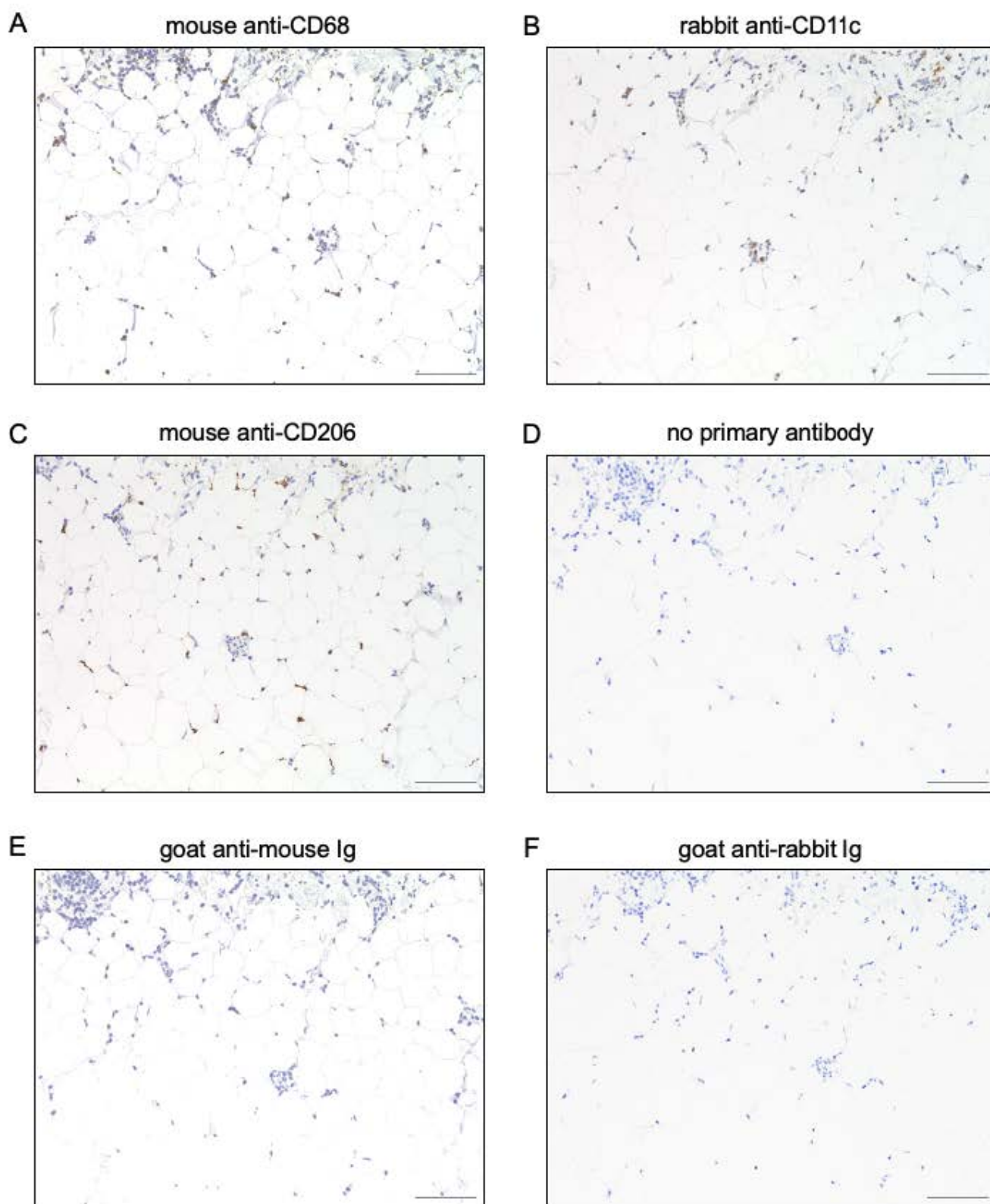


**Figure S1. Control experiments of immunohistological staining.**

**A-C.** Representative immunohistological staining using mouse anti-CD68 (A), rabbit anti-CD11c (B) and mouse anti-CD206 (C) primary antibodies in perivascular adipose tissue surrounding the aorta (Ao-PVAT). **D-F.** Representative immunohistological staining in the absence of a primary antibody (D) and using control primary antibodies of goat anti-mouse immunoglobulins (Ig) (E) and goat anti-rabbit Ig (F) in Ao-PVAT. Scale bar: 100  $\mu$ m.

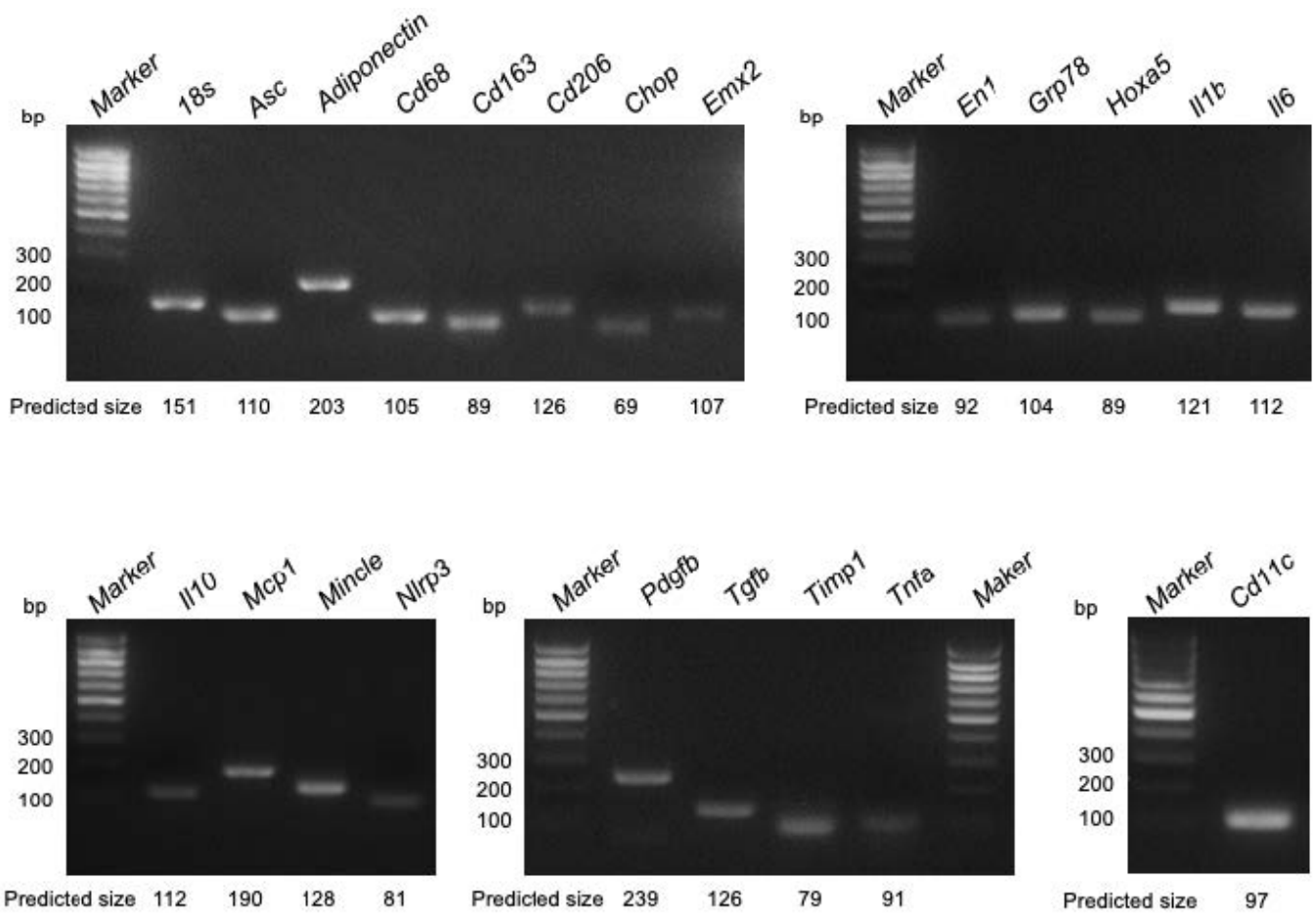


**Figure S2. Images of PCR amplicons in 2% agarose gels.**

The specificity of the PCR reaction of genes was confirmed by one distinct band, which matched with the predicted size of the PCR amplicon.